CDF/PUB/BOTTOM/PUBLIC/4433
Jan. 11, 1998

BEAUTIFUL PHYSICS AT CDF*

G. Bauer
(representing the CDF Collaboration)
Laboratory for Nuclear Science
Massachusetts Institute of Technology
Cambridge, Massachusetts, U.S.A.

Abstract

B-physics with $\bar{p}p$ collisions at CDF is reviewed, including production cross sections, masses, and decay properties. with a focus on lifetime and mixing measurements. A two-component lifetime fit of $B_s^0 \to \ell^+ D_s^- X$ results in the limit $\Delta\Gamma_s/\Gamma_s < 0.81$ (95% C.L.), which is converted into an indirect upper bound on Δm_s. From our five B_d^0-$\overline{B}_d^0$ oscillation analyses, we highlight the use of "same side" flavor tagging.

1 Introduction

B-physics at the Fermilab $\bar{p}p$-collider ($\sqrt{s}$ of 1.8 TeV) is an arena of special interest by virtue of the large cross section: at a typical luminosity of $10^{31}/\text{cm}^2/\text{s}$, b-quarks are produced at ~ 300 Hz. Unfortunately this corresponds to only about one interaction in a thousand. Furthermore, and unlike $Z^0 \to b\bar{b}$, the typical $p_T(b)$ is only a few GeV/c, making it difficult to select b's out of the large background. Despite this handicap, a broad range of topics may be studied: QCD tests of heavy quark production, b-hadron properties (masses, lifetimes,...), B^0-mixing, and before long, CP-violation.

The large backgrounds are suppressed by relying on the feature that heavy quarks produce relatively high p_T leptons, either through semileptonic decays, or via decays involving ψ's or Υ's which decayed into dileptons. The triggers used in the analyses presented here are, basically, inclusive single leptons (e, μ) with thresholds of about 8 GeV p_T, dimuons (2 GeV $p_T(\mu)$), and e-μ (5 and 2.5 GeV p_T). The implementation of the triggers [1, 2], as well as details of the CDF detector [3] are described in detail elsewhere; we only note that the detector now includes a Si-μvertex tracker (SVX) [4] capable of discerning displaced b-decay vertices.

*Talk given at the Beauty97 Workshop, Los Angeles, CA, October 13-17, 1997.

Several strategies are employed at CDF for b identification: secondary vertices, high p_T leptons, J/ψ's with a displaced vertex, semi-exclusive reconstructions via lepton+D, and full exclusive reconstruction of J/ψ modes. The data discussed here are from the Tevatron Run I (1992-96), and the analyses span integrated luminosities from $\sim$ 15–115 pb^{-1}.

2 b-Production

Hadronic production of heavy quarks is an important testing ground for perturbative QCD. The top quark opens a new window in this area, but detailed studies remain limited to charm and bottom. CDF has measured b cross sections (and production correlations) using: statistical separation of b's using impact parameters in inclusive jet ($E_T > 50$ GeV) events [5]; μ-b (correlated) cross sections [6]; μ-μ (correlated) cross sections [7]; semi-exclusive reconstruction (lepton+D) of B mesons [1, 5]; inclusive J/ψ cross sections [8]; exclusive B-reconstructions ($B \to J/\psi K^+$ and $J/\psi K^{*0}$) [9]; and from Υ's [10]. Each technique has its own complementary range in p_T and statistics, as well as the specificity of the produced hadron (generic b-hadron vs. specific B meson).

These analyses have largely been published and are not discussed here. We only note that the results are in reasonable agreement with the *shapes* calculated from next-to-leading order QCD, but the data are systematically higher ($\sim$ 2-3$\times$) than theory. This appears to be a general feature of our data, and, to a lesser degree, those of D0 [11] and UA1 ($\sqrt{s}$ = 630 GeV) [12]: both are $\sim 2 \times$ QCD. The CDF results are also higher than those from D0 and UA1. The situation has been recently reviewed in [13].

In order to check the $\sqrt{s}$ dependence, the Tevatron was operated at 630 GeV for a short time late in Run I, and the b cross section was measured using muons from secondary vertices. Many experimental and theoretical systematics cancel when taking the ratio of cross sections. So we express the result of this analysis as

$$\frac{\sigma(630)/\sigma(1800)|_{CDF}}{\sigma(630)/\sigma(1800)|_{QCD}} = 1.0 \pm 0.2,$$

showing that the $\sqrt{s}$-dependence observed by CDF is in good agreement with NLO QCD.

In this era of the "invincible" Standard Model, it is interesting to note that "mundane" studies of cross sections have provided one of the rare cases where a theoretical expectation has stumbled in dramatic fashion. Having for the first time a precision vertex detector in a hadron collider, CDF was able to separate the B contribution to J/ψ and ψ' from their direct production. This led to the striking discovery that direct production of the ψ' was $\sim 50\times$ larger than theoretical expectations, as shown in Fig. 1 [14]. CDF also found a similarly stark disagreement for J/ψ production, once $\chi \to J/\psi\gamma$ feed-down was removed. These results provoked a variety of hypotheses, the most popular probably being the "color octet" model [15]. We hope to soon have results on ψ polarization, which may shed more light on the production mechanisms.

3 b-Hadron Masses

CDF can measure b-hadron masses quite precisely from exclusive decays containing a J/ψ and charged tracks in the final state. This is an example where the high b rate pays off by producing

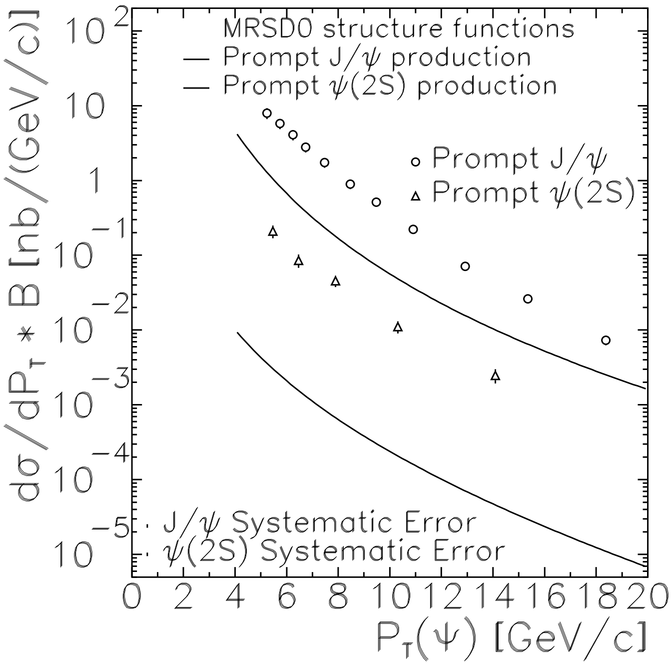

Figure 1: The J/ψ and $\psi(2S)$ cross sections with the B contribution removed; the theory curve is from the color singlet model [14].

large exclusive samples. Also important is the large sample of inclusive $J/\psi \rightarrow \mu^+\mu^-$ events which serves as a calibration tool.

Since these results have been published, we only summarize the results. In a ~ 19 pb^{-1} subset of data we reconstructed $B^+ \rightarrow J/\psi K^+$, $B_d^0 \rightarrow J/\psi K^{*0}$ ($K^{*0} \rightarrow K^+\pi^-$), and $B_s^0 \rightarrow J/\psi\phi$ ($\phi \rightarrow K^+K^-$). The masses were determined to be $m(B^+) = 5279.1 \pm 1.7 \pm 1.4$, $m(B_d^0) = 5281.3 \pm 2.2 \pm 1.4$, $m(B_s^0) = 5369.9 \pm 2.3 \pm 1.3$ MeV/c^2 (statistical followed by systematic errors) [16]. The precision for the non-strange mesons is not quite as good as other experiments, but the B_s^0 measurement is half the uncertainty of the next best [17].

We have also measured the mass of the Λ_b via the $J/\psi\Lambda$ ($\Lambda \rightarrow p\pi^-$) mode. For the full Run I sample 19.9 ± 6.4 candidates were fit to give a mass of $5621 \pm 4 \pm 3$ MeV/c^2 [18], a large improvement over other measurements[17].

4 B-Meson Decays

Measurements of event rates for exclusive decays may also be used to obtain relative branching ratios (Br). We have measured the branching ratios of $B_d^0 \rightarrow J/\psi K^0$, $B_d^0 \rightarrow J/\psi K^{*0}$, $B^+ \rightarrow J/\psi K^{*+}$, and $B_s^0 \rightarrow J/\psi\phi$, relative to $B^+ \rightarrow J/\psi K^+$ [19]. We have also observed the Cabbibo-suppressed decay $B^+ \rightarrow J/\psi\pi^+$. Its branching ratio relative to $J/\psi K^+$ was found to be $5.0^{+1.9}_{-1.7} \pm 0.1$ % [20], comparing well to CLEO's value of 5.2 ± 2.4 % [21].

Sensitive searches for a variety of rare decays are possible by virtue of their clean signatures. We have new results (100 pb^{-1}) on the FCNC $B_{d,s}^0 \rightarrow \mu^+\mu^-$. These are forbidden at tree level in the Standard Model, but at higher orders the branching fractions are expected to be about 10^{-10} and 10^{-9} for B_d^0 and B_s^0, respectively.

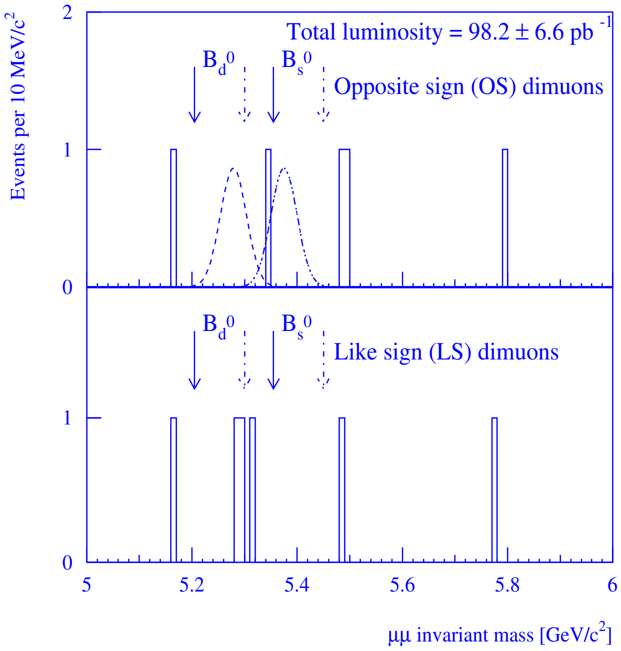

Figure 2: Dimuon masses from the $B \to \mu\mu$ selection. The arrows mark the $B^0_{s,d}$ windows. The dashed curves show the expected mass resolution for reconstructing B^0_d and B^0_s.

This search uses dimuon triggers and requires the kinematic cuts $p_T(\mu) > 2.0$ GeV/c and $p_T(\mu\mu) > 2.0$ GeV/c. Background is suppressed very effectively by requiring the $c\tau(\mu\mu) > 100\ \mu$m and that the dimuons be *isolated*, *i.e.*, $p_T(\mu\mu)/[p_T(\mu\mu) + \Sigma p_T] > 0.75$, where Σp_T is the scalar sum of track p_T's that lie in a η-ϕ cone of 1.0 around the muon pair. We define the B^0_d signal region to include events with masses between 5.205 and 5.355 GeV/c^2, and for B^0_s between 5.300 and 5.344 GeV/c^2. Figure 2 shows the mass distribution for opposite and like sign events. There is one opposite sign candidate (5.344 GeV/c^2) in the signal region, which happens to fall in the overlap region for both B^0_d and B^0_s. It is clearly consistent with background. However, to determine the branching fraction limit we count this event as a signal candidate. We find that $Br(B^0_d \to \mu^+\mu^-) < 6.8 \times 10^{-7}$ and $Br(B^0_s \to \mu^+\mu^-) < 2.0 \times 10^{-6}$ at 90% CL.

For 18 pb^{-1} of data we also have $Br(B^+ \to \mu^+\mu^- K^+) < 1.0 \times 10^{-5}$ and $Br(B^0_d \to \mu^+\mu^- K^{*0}) < 2.5 \times 10^{-5}$ at 90% CL [22].

We can search for some interesting non-leptonic modes which have distinctive characteristics to trigger on as well. A special "Penguin" trigger was devised late in Run I which triggered on a "photon" cluster above 10 GeV, plus two opposite sign tracks each with $p_T > 2$ GeV and in the vicinity of the "photon." For 23 pb^{-1} of data we find $Br(B^0_d \to K^{*0}\gamma) < 2.2 \times 10^{-4}$ (one candidate found), and $Br(B^0_s \to \phi\gamma) < 3.9 \times 10^{-4}$ (no candidates) at 90% CL. The B^0_d limit is a factor of 5 larger than CLEO's observation at $\sim 4 \times 10^{-5}$ [23], but it illustrates the use of specialized non-leptonic triggers to access interesting modes in a hadron collider. The B^0_s limit is comparable to LEP values [24].

Table 1: B-meson lifetimes (ps) and ratios (first error is statistical, second systematic).

Lifetime	Exclusive	Semi-Exclusive	World Averages [17]
τ_u^+	$1.68 \pm 0.07 \pm 0.02$	$1.64 \pm 0.06 \pm 0.05$	1.64 ± 0.05
τ_d^0	$1.58 \pm 0.09 \pm 0.02$	$1.48 \pm 0.04 \pm 0.05$	1.55 ± 0.05
τ_u^+/τ_d^0	$1.06 \pm 0.07 \pm 0.02$	$1.11 \pm 0.06 \pm 0.03$	1.03 ± 0.05
τ_s^0	$1.34\ {}^{+0.23}_{-0.19} \pm 0.05$	$1.39 \pm 0.09 \pm 0.05$	1.57 ± 0.08
$\tau_{\Lambda b}^0$	–	$1.32 \pm 0.15 \pm 0.07$	$1.11\ {}^{+0.13}_{-0.12}$

5 b-Hadron Lifetimes

Lifetime differences are governed by details of the decay mechanisms beyond the naive spectator model. In contrast to D^+/D^0, small differences ($\sim$ 5-10%) are expected between B^+ and B_d^0, and virtually no difference between B_s^0 and B_d^0, thereby demanding excellent precision [25].

We recently submitted our final Run I exclusive B lifetimes using $B^+ \to J/\psi K^+$, $B_d^0 \to J/\psi K^{*0}$, and $B_s^0 \to J/\psi\phi$ for publication [26], and they are listed in Table 1. These exclusive modes have small systematic errors, unfortunately the statistical errors are much larger.

Larger statistical samples may be obtained by utilizing semi-exclusive decays $B_{u,d,s} \to \ell D^{(*)} X$, where $\ell = e, \mu$, and the "$D^{(*)}$" is reconstructed in a cone around the lepton via

$$
\begin{array}{lll lll}
D^0 & \to & K^-\pi^+ & & & \\
D^{*+} & \to & D^0\pi_*^+ & D^0 & \to & K^-\pi^+ \\
 & & & & \to & K^-\pi^+\pi^0_{lost} \\
 & & & & \to & K^-\pi^+\pi^+\pi^- \\
D_s^- & \to & \phi\pi^- & \phi & \to & K^+K^- \\
 & \to & \phi\mu^- X & \phi & \to & K^+K^- \\
 & \to & K^{*0}K^- & K^{*0} & \to & K^+\pi^- \\
 & \to & K_s^0 K^- & K_s^0 & \to & \pi^+\pi^-
\end{array}
$$

The B-decay vertex is determined from the intersection of the lepton and D trajectories. The exact $\beta\gamma$-factor to convert the decay distance into $c\tau$ is unknown because of missing particles. An average $\beta\gamma$ correction is derived from Monte Carlo (observed $p_T(\ell D)$ is $\sim$ 85% of the true value), and applied to the data [27].

A second complication arises because imperfect reconstruction introduces cross-talk between the B^+ and B^0 reconstructions. For example, $\ell^+\overline{D}^0$ is nominally from a B^+, but could really have been $B_d^0 \to \ell^+\overline{D}^{**-}$ where $D^{**-} \to \overline{D}^0\pi_{**}^-$ and the soft π_{**}^- is lost. The cross talk among decay modes is largely constrained from known branching ratios and isospin arguments. Very poorly known quantities—like the relative rate of $D^{**} \to D^*\pi_{**}$ compared to $D\pi$—are allowed to span the full range. We find that the $\ell^+\overline{D}^0$ channel is about 85% B^+ and ℓ^+D^{*-} is about 90% B^0. Since the B^+ and B_d^0 lifetimes are so similar, the results are in fact not very sensitive to the cross-talk. However, in the ratio τ_u^+/τ_d^0, the sample composition is the largest systematic. Table 1 lists the results.

A parallel semileptonic analysis for B_s^0 has recently been improved by adding the D_s^- decays to $K^{*0}K^-$, $K_s^0K^-$, and $\phi\mu^-X$ to our original sample of $\phi\pi^-$. The combined semileptonic B_s^0 lifetime is $1.39 \pm 0.09 \pm 0.05$ ps.

A similar measurement for the Λ_b^0 via $\ell^-\Lambda_c^+$ ($\Lambda_c^+ \to pK^-\pi+$) yields a lifetime $1.32 \pm 0.15 \pm 0.07$

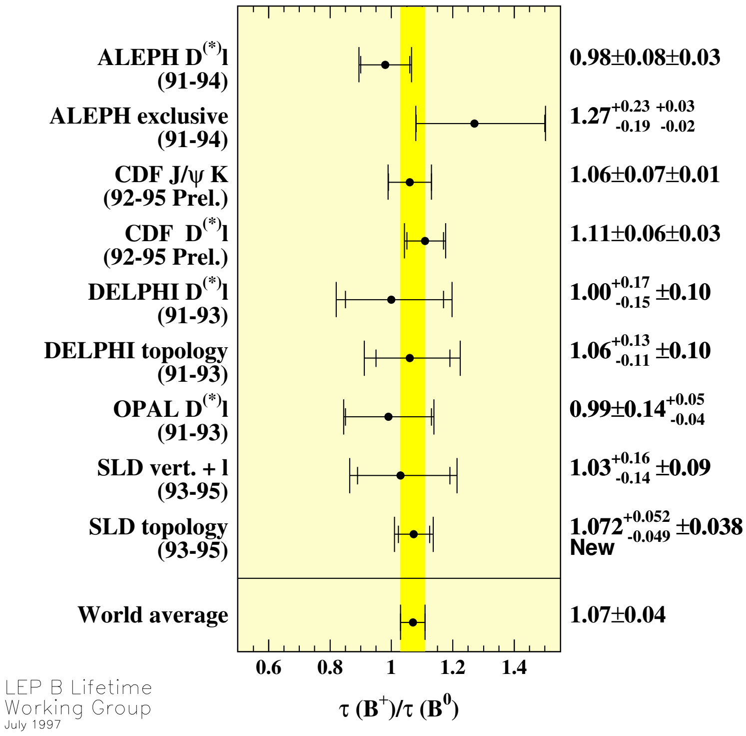

Figure 3: A recent compilation of B^+/B_d^0 lifetime ratios, and average value [30].

ps for 110 pb^{-1} [28]. Our result is on the high side of the world average, but the shortness of the world average lifetime remains unexplained [25].

The exclusive modes have small systematic errors, but "large" statistical ones, whereas the situation is reversed for the semileptonic results. The dominant contributions to the semileptonic systematics come from the approximate $\beta\gamma$ corrections, and the poorer B vertex resolution from pointing the D back to a single track, the lepton. The exclusive modes will provide extremely precise values with ~ 2 fb^{-1} data sets available in Run II [29]. Our results compare well, both in value and sensitivity, with world averages (Table 1). As an example, our B^+/B_d^0-lifetime ratios are shown in Fig. 3 along with other experiments from a compilation by the LEP B Lifetime Working Group [30]. The average of the B^+/B_d^0 ratio—dominated by four results, the two from CDF and one each from ALEPH and SLD—is 1.07 ± 0.04, a small difference, if any, as expected.

The B_s^0 measurements are very close to the B_d^0, as expected [25]. The B_s^0 lifetime is of interest for reasons beyond searching for non-spectator effects. Since B_s^0 mixing is known to be large ($\Delta m_s > 10$ ps^{-1}[31]), the oscillation is very rapid, and it may not be feasible to observe the oscillation as has been done for the B_d^0. However, this may mean that the two CP-eigenstates may have significantly different lifetimes, *i.e.*, $\Delta\Gamma_s/\Gamma_s$ may be large. The $B_s^0 \to J/\psi\phi$ is expected to be (mostly) CP-even, whereas the semileptonic $\ell^+ D_s^-$ is an equal mixture of even and odd. Therefore these two modes could have different lifetimes, or a second lifetime component may be visible in $\ell^+ D_s^-$.

Although our $J/\psi\phi$ measurement is unique, the statistics are woefully inadequate to make any meaningful comparison with the $\ell^+ D_s^-$ lifetime. However, the greater statistics in Run II will make this an interesting comparison.

While the $J/\psi\phi$ is statistically inadequate to look for a lifetime difference, we have looked for two lifetime components within the $\ell^+ D_s^-$ sample. Instead of fitting the B_s^0 lifetime distribution to the usual mean lifetime form, $\exp(-t/\tau_{mean})$, we fit in terms of the light and heavy CP-eigenstate widths ($\Gamma_{L,H} = \Gamma \pm \Delta\Gamma$), *i.e.*,

$$\frac{1}{2}\Gamma\left(1+\frac{\Delta\Gamma}{2\Gamma}\right)e^{-\Gamma(1+\frac{\Delta\Gamma}{2\Gamma})t}+\frac{1}{2}\Gamma\left(1-\frac{\Delta\Gamma}{2\Gamma}\right)e^{-\Gamma(1-\frac{\Delta\Gamma}{2\Gamma})t}.$$

However, since the mean lifetime and mean width are not inverses, and we wish to take advantage of the precise world mean lifetime, we recast this function so that τ_{mean} and $\Delta\Gamma/\Gamma$ are the two independent parameters.

The fit of our ℓD_s events, fixing τ_{mean} to the world average 1.57 ± 0.08 ps [17], yields $\Delta\Gamma/\Gamma = 0.48^{+0.26}_{-0.48}$, and corresponds to $\Delta\Gamma/\Gamma < 0.81$ at 95% CL. This can be expressed as an upper bound on Δm_s, given $\Delta\Gamma/\Delta m$ and τ_{mean},

$$\Delta m_s < 92\,\mathrm{ps}^{-1} \times \left(\frac{5.6\times 10^{-3}}{\Delta\Gamma/\Delta m}\right)\left(\frac{1.57\mathrm{ps}}{\tau_{mean}}\right)$$

at 95% C.L. The constant coefficient, $92\,\mathrm{ps}^{-1}$, is then the limit obtained for the mean lifetime $\tau(B_s^0) = 1.57$ ps, and for $\Delta\Gamma/\Delta m = 5.6 \times 10^{-3}$, a recent estimate [32].

6 B^0-$\bar{B}^0$ Mixing

As is the case in the K^0-system, higher order weak interactions are responsible for $B^0 \leftrightarrow \overline{B}^0$ transitions which result in mass eigenstates (B^0_{Heavy} and B^0_{Light}) that are a mixture of weak eigenstates (B^0 & $\overline{B}^0$). A consequence of this is that a B^0 (produced at time $t = 0$) will turn into a $\overline{B}^0$ (at time t) with a probability

$$\mathcal{P}(B^0(t=0) \to \overline{B}^0(t)) \;=\; \frac{e^{-t/\tau}}{2\tau}[1-\cos(\Delta m t)]$$

where τ is the (average) B lifetime and $\Delta m \;=\; m(B^0_H) - m(B^0_L)$. The time-dependence can be integrated out to yield the overall probability for a produced B^0 to be observed as a $\overline{B}^0$:

$$\mathcal{P}(B^0 \to \overline{B}^0) \;\equiv\; \chi \;=\; \frac{x^2}{2(1+x^2)}$$

with $x \equiv \Delta m/\Gamma$, and Γ the (average) width.

The key ingredient to observe mixing is establishing the production and decay flavors of the B^0's (*i.e.*, whether it contained a b or $\bar{b}$). Mixing in the B^0-systems was first seen ten years ago by UA1 [33] in a time-integrated measurement using the charge correlation of dimuons. CDF has used this technique to determine χ averaged over B_d^0 and B_s^0 for μ-μ ($0.131 \pm 0.020 \pm 0.016$ [7]) and e-μ ($0.130 \pm 0.010 \pm 0.009$ [34]) events.

The χ-type analysis has been overshadowed by the direct observation of the time-dependence of the B_d^0-$\overline{B}_d^0$ oscillation, first demonstrated by ALEPH [35]. The flavor oscillation is observed as an asymmetry in the number of mixed ($N_M(t)$) and unmixed B^0's ($N_U(t)$) as a function of time,

$$\mathcal{A}^0(t) = \frac{N_U(t) - N_M(t)}{N_U(t) + N_M(t)} = \cos(\Delta m_d t).$$

However, if the tagging method correctly identifies the flavor with a probability of only P_0, then the amplitude of the observed asymmetry, $\mathcal{A}^0_m(t)$ is reduced by the "dilution" factor $\mathcal{D}_0 \equiv 2P_0 - 1$, so that $\mathcal{A}^0_m(t) = \mathcal{D}_0 \cos(\Delta m_d t)$. The figure of merit for the power of a tagging method is its *effective tagging efficiency*, $\varepsilon\mathcal{D}^2$, where ε is just the tagging efficiency.

CDF currently has five oscillation measurements of Δm_d. We will feature one of them, selected for its novel tagging method, and the fact that it has our largest $\varepsilon\mathcal{D}^2$ (although it does not yield the most precise Δm_d). B samples will grow dramatically in the coming years, but the desire to flavor tag ever rarer processes for CP-violation studies begs for the development of all means that can be brought to bear.

6.1 Observation of Flavor Oscillations Using SST

Most flavor tagging techniques rely upon inferring the initial flavor of one B meson by determining the decay flavor of the other b-hadron in the event, such as dilepton charge correlations or away-side jet charge. We classify these approaches as *Opposite Side Tagging* (OST). However, Gronau, Nippe, and Rosner [36] suggested that one might be able to use correlations between the B and charged particles produced along with it. This could arise from fragmentation particles as well as from the decays of B^{**} mesons. If we naively consider a $\bar{b}$ fragmenting into a B^0, it must pick up a d, which leaves a $\bar{d}$. To make a charged pion, the $\bar{d}$ must pick up a u, resulting in a B^0-π^+ pair. On the other hand, if the $\bar{b}$ is to make a B^+, the associated pion will be a π^-. The same correlation arises from $B^{**+} \to B^{(*)0}\pi^+$ and $B^{**0} \to B^{(*)+}\pi^-$.

Our "Same Side Tagging" (SST) method [37] exploits these correlations, but we neither distinguish the source of the pions, nor if they are indeed pions. They may be kaons or even protons, but will generically be referred to as "pions." Note that in order to use the tag sign, it is necessary to know if the B is charged or neutral.

We select our SST track by considering all charged tracks that lie in a cone $\Delta R = \sqrt{(\Delta\eta)^2 + (\Delta\phi)^2}$ ≤ 0.7 centered along the reconstructed B direction, have $p_T > 400$ MeV/c, and are from the primary vertex. This last requirement is principally that the track's (transverse) impact parameter significance is less than 3σ. If more than one candidate qualifies, the one with the *smallest* p_T^{rel} is selected, *i.e.*, the one with the smallest momentum component transverse to the track-B system $(\vec{p}_{TR} + \vec{p}_B)$.

The B sample used is similar to the $\ell D^{(*)}$ lifetime analysis, but with the following decays,

$$
\begin{aligned}
B^0 &\to \nu\ell^+ D^{*-}, D^{*-} \to \overline{D^0}\pi^-_*, \overline{D^0} \to K^+\pi^- \\
B^0 &\to \nu\ell^+ D^{*-}, D^{*-} \to \overline{D^0}\pi^-_*, \overline{D^0} \to K^+\pi^-\pi^-\pi^+ \\
B^0 &\to \nu\ell^+ D^{*-}, D^{*-} \to \overline{D^0}\pi^-_*, \overline{D^0} \to K^+\pi^-\pi^0 \\
B^0 &\to \nu\ell^+ D^-, D^- \to K^+\pi^-\pi^- \\
B^+ &\to \nu\ell^+ \overline{D^0}, \overline{D^0} \to K^+\pi^-.
\end{aligned}
$$

The charm mass distributions are shown in Fig. 4, and are seen to be clean B samples with no excess in the "wrong sign" $(\ell^\pm K^\mp)$ ℓ+charm events (dashed histograms in Fig. 4).

In principle we can tag these events, determine the proper time of decay, and fit the time dependent asymmetry for Δm_d. However, the incomplete reconstruction of the B's introduces several complications: a) missing decay products means we do not know the precise $\beta\gamma$ factor; b) we *may* have missed a charged decay product, so what looks like a B^0 may really be a B^+; and

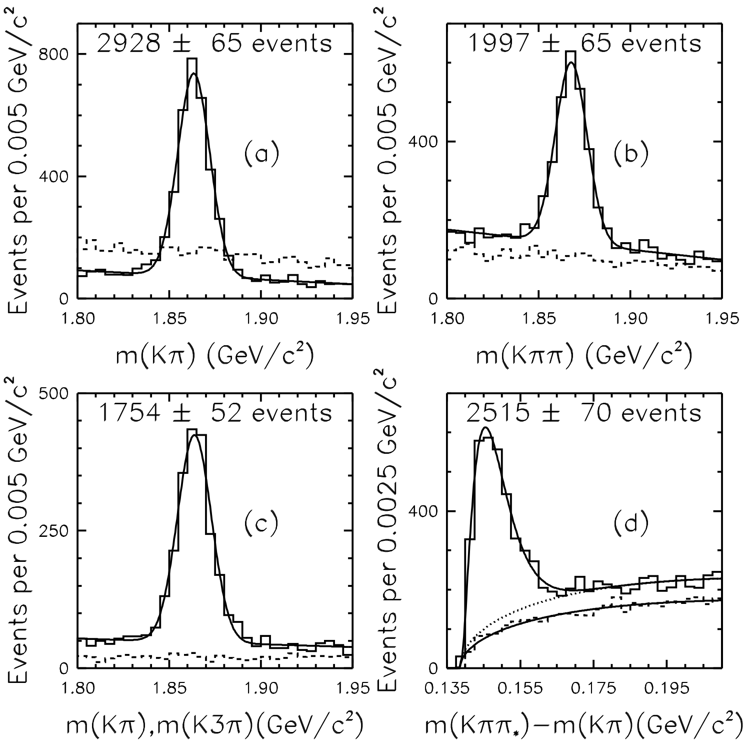

Figure 4: The mass distributions for ℓD samples: a) $K^+\pi^-$ mass for $\ell^+\overline{D}^0$; b) $K^+\pi^-\pi^-$ mass for ℓ^+D^-; c) $K^+\pi^-$ plus $K^+\pi^-\pi^+\pi^-$ masses for ℓ^+D^{*-} ($\overline{D}^0\pi_*^-$); d) $K^+\pi^-\pi_*^- - K^+\pi^-$ mass difference for ℓ^+D^{*-} ($D^{*-}\to\overline{D}^0\pi_*^-$, $\overline{D}^0\to K^+\pi^-\pi^0$, π^0 is lost). The dashed lines are for the wrong sign ($\ell^\pm K^\mp$) events, which is rescaled to the dotted line in d as the background.

c) a missing charged decay product might be chosen as the tag, and bias the observed asymmetry. The first two points are familiar from the $\ell D^{(*)}$ lifetime analysis. The $\beta\gamma$ corrections are handled in essentially the same way by Monte Carlo The B^0-B^+ cross-talk corrections—critical in a mixing analysis since B^0's and B^+'s have the *opposite* sign tags—use some of the basic elements of the lifetime analysis, but with a more sophisticated treatment and using additional constraints from the data [38].

The final subtlety is the prospect of tagging on one of the unidentified B decay products, namely the $\pi_{**}^\pm$'s from $B\to D^{**}\to D^{(*)}\pi_{**}$. This is especially important because the π_{**} charge *always* has the right sign correlation with the lepton, causing the observed asymmetry to be higher than the true asymmetry. The probability of getting such a tag depends upon branching ratios (how many $\pi_{**}^\pm$ are present), and the probability, ξ, to tag on a π_{**} given one *was* produced. The latter factor depends details of the decay kinematics and geometry, especially the proper decay distance, ct, and on the spectrum of fragmentation tracks. We use a Monte Carlo simulation to model the B decay kinematics and geometry—something it can do well—to obtain the ct shape of ξ. The normalization of ξ is determined from the data itself, and thus we do *not* rely on the simulation's description of the fragmentation tracks.

The effects of sample composition, tagging on $\pi_{**}^\pm$'s, and lifetime corrections are condensed into weighting factors for the various contributions to the asymmetry at a given ct, such as the B^0 asymmetry contribution $\mathcal{D}_0\cos(\Delta m_d t)$. Each of the five ℓD decay signatures has its own set

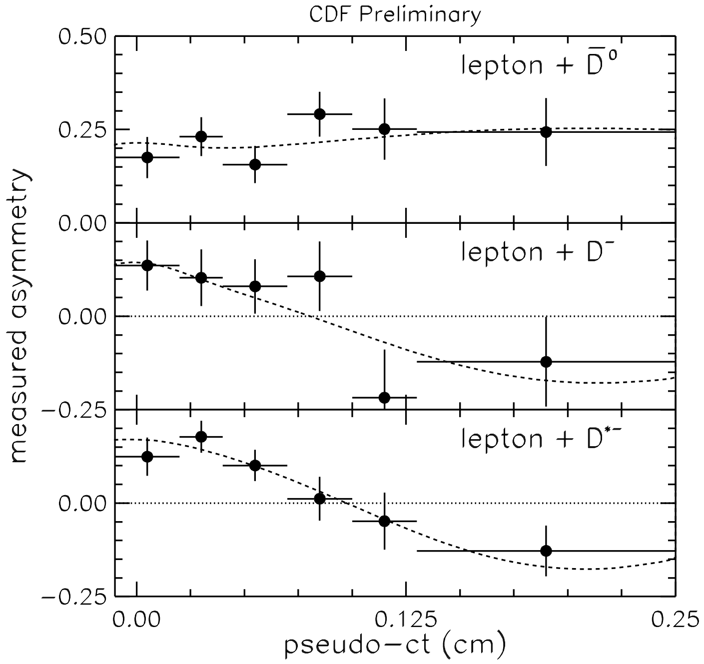

Figure 5: Measured flavor asymmetries as a function of proper decay length for, from top to bottom: $\ell^+\overline{D}^0$, $\ell^+\overline{D}^-$, and sum of all three $\ell^+\overline{D}^{*-}$ decay signatures. The $\ell^+\overline{D}^0$ is dominated by B^+'s, and the other two by B_d^0. The dashed curves represent simultaneous fit results.

of weights. This collection of weighting factors and true asymmetries allows us to compute the expected asymmetry in a ct-bin for each decay signature. We form a χ^2 function to simultaneously fit the observed asymmetries to the "predictions" in bins of ct for each B-subsample.

The weighting factors depend on the sample composition, π_{**} tag rate, and other parameters, often in complicated ways. Some of these input parameters are not well known, or can be constrained by the data itself. We therefore make these parameters part of the fit by adding a term to the χ^2 function for each one based on a measured value and error for it. These input parameters are then allowed to float within their uncertainties, and affect the asymmetry weights which are functions of them [38].

The principle free parameters of the fit are Δm_d (frequency of the B^0 oscillation), the B^0 dilution (the amplitude of the oscillation), and the B^+ dilution (magnitude of the B^+-π^- correlation). The measured asymmetries are plotted in Fig. 5 along with the results of the fit. The lower two plots are predominately B^0, with clear oscillations. The top plot is mostly B^+, and is consistent with being flat. The small wiggle present in the fit function reflects the small B^0 contamination present in this case. The lower plots also have B^+ contamination, but being simply a constant shift, it is not apparent.

The fit results, including the errors on the sample composition parameters, external parameters from other sources, and residual backgrounds, yields the mixing frequency of

$$\Delta m_d = 0.471\ ^{+0.078}_{-0.068}\,(stat)\ \pm 0.034\,(sys)\ \mathrm{ps}^{-1}.$$

The amplitude of the observed asymmetry (corrected for sample composition) is also returned by the fit, and is simply the tagging dilution:

$$\begin{aligned}\mathcal{D}_+ &= 0.27 \pm 0.03 \pm 0.02 \\ \mathcal{D}_0 &= 0.18 \pm 0.03 \pm 0.02\end{aligned}$$

and, combined with the tagging efficiencies, ε, give

$$\begin{aligned}\varepsilon\mathcal{D}_+^2 &= (5.2 \pm 1.2^{+0.9}_{-0.6})\% \\ \varepsilon\mathcal{D}_0^2 &= (2.4 \pm 0.7^{+0.6}_{-0.4})\%.\end{aligned}$$

The errors are fairly large, but so far this method has the largest effective efficiency of all our tagging methods. SST is also well suited for tagging exclusive decay modes, which are currently under study.

6.2 CDF Average Δm_d

The SST analysis is only one of five CDF measurements of Δm_d, and not the most precise. As shown in Fig. 6, we also have results on the traditional dilepton charge correlations with μ-μ and e-μ, lepton plus away side lepton+charm, and finally lepton plus away side jet-charge or plus soft lepton tag (SLT). Combining all five results, the CDF average is $\Delta m_d = 0.474 \pm 0.029 \pm 0.026$ ps^{-1}. This compares very well with the 1997 PDG value of 0.484 ± 0.026 ps^{-1} [17].

7 Summary

Various facets of particle physics have been studied via b-quarks at CDF, from QCD tests of heavy quark production, masses, decay characteristics, lifetimes, to B^0-mixing. Many of these results are the most precise from a single experiment. Some of our results are now final, but the Run I data set is not yet exhausted. Since the Workshop, we have obtained new results on branching ratios of $B \to \psi' K$ decay modes, and expect in the near future to present results on B^{**}'s, extending the B_c^+ search from $J/\psi\pi^+$ [20] to the higher rate $J/\psi\ell^+\nu$ mode, and further mixing/tagging results.

On the more distant horizon, CDF is in the process of upgrading for the Main Injector run at the close of the millennium. Integrated data sets of order 2 fb^{-1} are expected, with which a high priority will be CP-violation studies. Progress and plans for the CDF II upgrade program are discussed in [29].

Acknowledgments: I would like to thank the organizers and staff of this conference for their hard work, and my fellow collaborators for the pleasure of representing them and their work. Special thanks to P. Maksimović, M. Paulini, K. Kordas, J. Kroll, J. Tseng, and A.B. Wicklund for their comments.

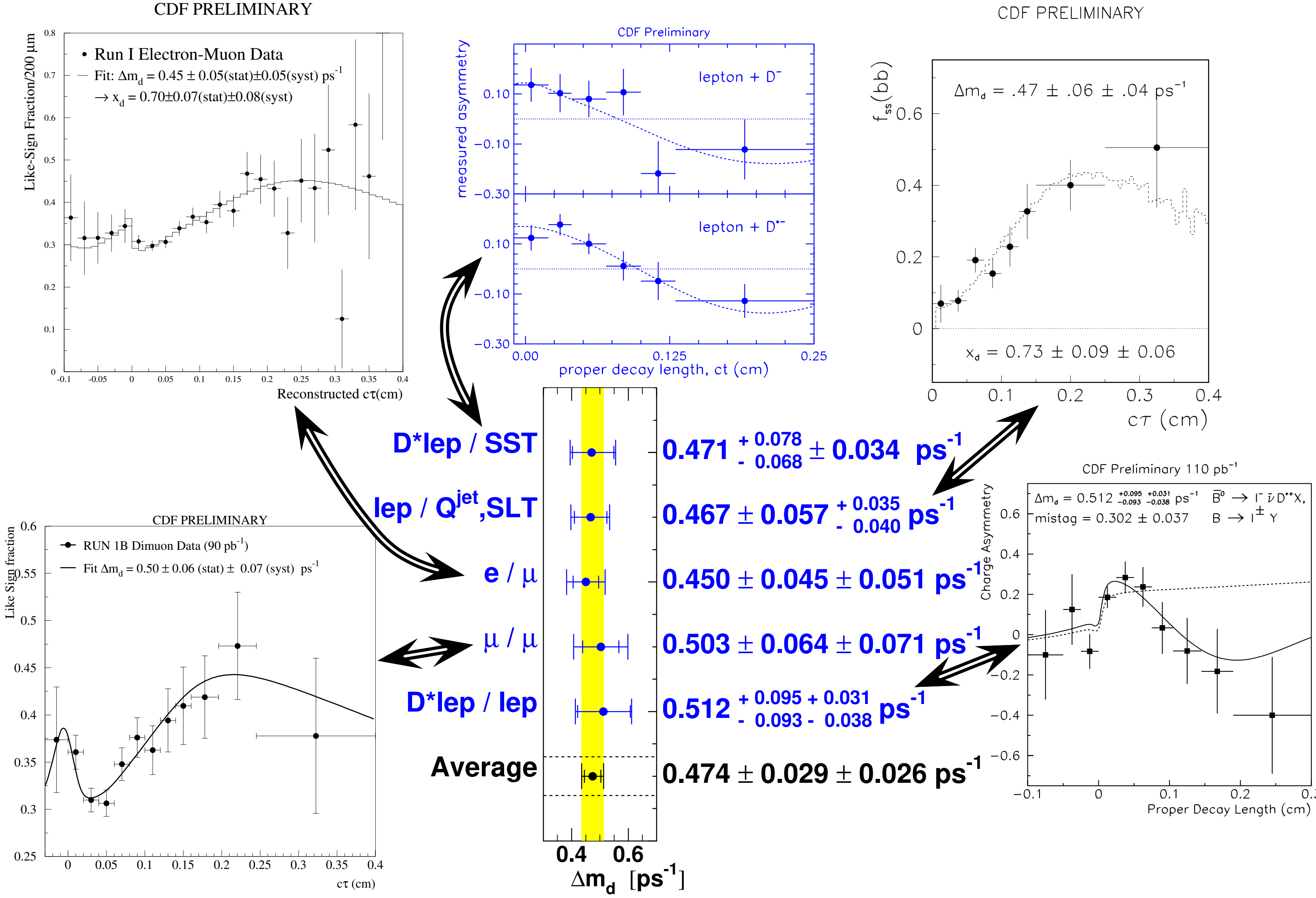

Figure 6: Five CDF B_d^0-oscillation measurements of Δm_d, and the combined average (see text).

Figure 6: Five CDF B_d^0-oscillation measurements of Δm_d, and the combined average (see text).

References

[1] F. Abe *et al.*, Phys. Rev. Lett. **71** (1993) 500.
[2] F. Abe *et al.*, Phys. Rev. Lett. **71** (1993) 3421; Phys. Rev. **D50** (1994) 2966.
[3] F. Abe *et al.*, Nucl. Instrum. Methods **A271** (1988) 387.
[4] D. Amidei *et al.*, Nucl. Instrum. Methods **A350** (1994) 73; P. Azzi *et al.*, Nucl. Instrum. Methods **A360** (1995) 137.
[5] P. Lukens, Proc. of *10th Topical Workshop on Proton-Antiproton Collider Physics*, Batavia, 1995, ed. R. Raja and J. Yoh, (AIP Conf. Proc. 357, 1996).
[6] F. Abe *et al.*, Phys. Rev. **D53** (1996) 1051.
[7] F. Abe *et al.*, Phys. Rev. **D55** (1997) 2546.
[8] F. Abe *et al.*, Phys. Rev. Lett. **79** (1997) 572.
[9] F. Abe *et al.*, Phys. Rev. Lett. **75** (1995) 1451.
[10] F. Abe *et al.*, Phys. Rev. Lett. **75** (1995) 4358.
[11] M. Baarmand, these proceedings.
[12] C. Albajar *et al.*, Phys. Lett. **213B** (1988) 405; **256B** (1991) 121.
[13] S. Frixione *et al.*, CERN-TH/97-16.
[14] K. Byrum *Proc. of the XXVII Conf. on High Energy Physics*, Glasgow, 1994, ed. P.J. Bussey and I.G. Knowles, (IOP, London, 1995); F. Abe *et al.*, Phys. Rev. Lett. **79** (1997) 572, and 578.
[15] G.T. Bodwin, E. Braaten, and G.P. Lepage, Phys. Rev. **D46** (1992) 1914; E. Braaten and S. Fleming, Phys. Rev. Lett. **74** (1995) 3327.
[16] F. Abe *et al.*, Phys. Rev. **D53** (1996) 3496.
[17] R.M. Barnet *et al.*, Particle Data Group, 1997 offyear update (http://pdg.lbl.gov/).
[18] F. Abe *et al.*, Phys. Rev. **D55** (1997) 1142.
[19] F. Abe *et al.*, Phys. Rev. **D54** (1996) 6596.
[20] F. Abe *et al.*, Phys. Rev. Lett. **77** (1996) 5176.
[21] M. Bishai *et al.*, Phys. Lett. **B369** (1996) 186.
[22] F. Abe *et al.*, Phys. Rev. Lett. **76** (1996) 4675.
[23] R. Ammar *et al.*, Phys. Rev. Lett. 71 (1993) 674.
[24] A.M.Litke, *Proc. of the XXVII Conf. on High Energy Physics*, Glasgow, 1994, ed. P.J. Bussey and I.G. Knowles, (IOP, London, 1995); W. Adam *et al.*, Zeit. Phys. C **72** (1996) 207.
[25] I. Bigi *et al.*, *B Decays*, Rev. 2nd Edition, ed. by S. Stone (World Scientific, Singapore, 1994), p.132.
[26] F. Abe *et al.*, FERMILAB-PUB-97/352-E, submitted to Phys. Rev. D.
[27] F. Abe *et al.*, Phys. Rev. Lett. **76** (1996) 4462.
[28] F. Abe *et al.*, Phys. Rev. Lett. **77** (1996) 1439.
[29] N. Lockyer, these proceedings.
[30] LEP B Lifetime Working Group, `http:// www.cern.ch/~claires/lepblife.html`.
[31] LEP B Mixing Working Group, `http:// www.cern.ch/LEPBOSC/`.
[32] M. Beneke, G. Buchalla, and I. Dunietz, Phys. Rev. **D54** (1996) 4419.
[33] C. Albajar *et al.*, Phys. Lett. **B186** (1987) 247.
[34] F. Abe *et al.*, FERMILAB-CONF-95/230-E.
[35] D. Buskulic *et al.*, Phys. Lett. **B313** (1993) 498.
[36] M. Gronau, A. Nippe, and J.L. Rosner, Phys. Rev. **D47** (1993) 1988.
[37] F. Abe *et al.*, FERMILAB-PUB-97/312-E, submitted to Phys. Rev. Lett.
[38] P. Maksimović, Ph.D. dissertation, Mass. Inst. of Tech., 1998.